5th Australasian Congress on Applied Mechanics, ACAM 2007
10-12 December 2007, Brisbane, Australia

Hysteretic Damping of Shear Panel Energy Dissipater

Ricky WK Chan[1], Faris Albermani[1] and Martin S. Williams[2]

[1]*Department of Civil Engineering, University of Queensland, Australia*
[2]*Department of Engineering Science, Oxford University, UK*

Abstract: This paper describes an experimental investigation of a new earthquake damper for civil structures. It utilizes the energy dissipative capability of plastic shear deformation of thin steel plates welded inside a standard SHS steel section. Its performance is verified by fifteen cyclic and monotonic tests. Experiments showed that this light-weight damper exhibited stable behavior and was capable of dissipating a significant amount of energy. Its performance is influenced by the plate slenderness ratio and by the rigidity of its boundary elements. Slender plates buckled in shear, causing pinching of the hysteresis loop without significant strength degradation. The magnitude of damping offered by the dissipater is quantified. Fabrication, implementation and replacement of the damper proved to be easy and inexpensive. The seismic performance of a structure equipped with shear panel dissipaters is demonstrated using a numerical example.

Keywords: passive energy dissipation, cyclic test, earthquake engineering.

1 Introduction

Interest in the development of passive energy dissipation in earthquake risk mitigation of civil structures has greatly increased in the last two decades [1]. During an event of earthquake, a large amount of energy is imparted to a structure. Traditional design approach relies on the energy dissipation as a consequence of inelastic deformation of particular structural zones. The permanent damage of post-disaster structures are often so serious that it would be expensive to repair, even if it is possible. The concept of passive energy dissipation, however, attempts to reduce such permanent damage to the structure. With designated energy dissipative devices installed within a structure, a portion of the input seismic energy could be diverted into these devices; as a result damage of the parent structure can be effectively reduced. In addition, by locating these devices at convenient positions, repair and/or replacement of the devices after earthquakes can be carried out with minimal interruption to occupancy, a crucial benefit to building owners and occupants.

A number of dissipative devices utilize plastic deformation of metals have been proposed. Devices which make use of flexural deformation of metals include the patented ADAS [2], its variant TADAS [3] and the Slit Damper, SD [4]. The Buckling-restrained brace BRB [5], on the other hand, makes use of the axial deformation of a steel member. Recently, the energy dissipative capability of inelastic shear deformation of steel plate has been investigated. Nakashima et al [6] tested the Low Yield Steel Shear Panel (LYSSP) and reported very stable hysteresis behavior. A few field implementations of shear panel have been reported in Japan [7].

The Yielding Shear Panel Device (YSPD), first proposed by Schmidt et al [8], utilizes the inelastic shear deformation of steel plate to dissipate input energy. Williams et al [9] tested a steel frame fitted with YSPD of various thicknesses and concluded that the device dissipates a significant amount of input energy. In this research, devices are tested on an isolated test setup. This paper first discusses the preliminary design of the device, followed by experimental and numerical verifications.

2 Yielding Shear Panel Device (YSPD)

Figure 1 (a) shows the yielding shear panel device tested in this research. It is fabricated using a short segment of a square hollow section (SHS, dimension *DxD*) with a steel diaphragm plate (thickness *t*) welded inside it. In this research, the length of the SHS section is chosen to equal its width (i.e. *D*). Four bolt holes (spaced at 50mm) are drilled on each of the two opposite SHS flanges for the connection to the test setup. Relative horizontal displacement between the top and bottom connections causes the diaphragm plate to deform in shear. When the displacement is sufficiently large the plate deforms plastically, and as a result input energy is dissipated. Fabrication and installation of the device is simple and inexpensive.

2.1 Preliminary design of YSPD

Neglecting the contribution of the SHS, the theoretical elastic in-plane stiffness of the device k_d is given by,

$$k_d = Gt \tag{1}$$

where G is shear modulus and t is the thickness of the diaphragm plate. For a compact diaphragm plate the yield strength of the device can be taken as the shear yield strength of the plate,

$$F_y = \frac{f_y}{\sqrt{3}} dt \tag{2}$$

Consequently the yield displacement of the device is,

$$u_y = \frac{F_y}{k_d} = \frac{f_y d}{\sqrt{3}G} \tag{3}$$

For a device with a slender diaphragm plate, elastic shear buckling will take place. The critical shear stress for a simply supported plate is given by,

$$\tau_{cr} = k_s \frac{\pi^2 E}{12(1-\nu^2)} \left(\frac{t}{d} \right)^2 \tag{4}$$

where k_s depends on the aspect ratio of the plate, and equals to 9.35 for square plates. E and ν are Young's modulus and Poisson's ratio respectively. Taking $\nu = 0.3$ and $E = 205GPa$, the limiting plate slenderness ratio at which buckling controls is $d/t = 1732/\sqrt{f_y}$, where f_y is the tensile yield strength of the diaphragm plate (MPa).

2.2 Experimental verification

Performance of passive energy devices are influenced by many factors such as connection details, surrounding structural elements and possible flaws in fabrication. Therefore, it is essential to conduct a testing program to verify the cyclic performance and energy dissipation capacity of the proposed YSPD.

2.3 Specimens

Twelve specimens similar to Figure 1(a) were fabricated at the structures laboratory of the City University of Hong Kong. The diaphragm plate was first positioned inside the SHS, spot-welded at four corners and subsequently welding is applied along perimeter of plates on both sides. Two sizes of SHS (100x100x4 and 120x120x5) and three diaphragm plate thicknesses (2, 3, and 4mm) were used, resulting in six different diaphragm plate-to-SHS combinations. The following notation is adopted to identify different specimens used in the test: *D-tM* or *D-tC*, where *D* indicates the size of the SHS section (either 100 or 120mm), *t* is the thickness of the diaphragm plate (2, 3 or 4 mm). The letter *M* indicates monotonic while *C* is cyclic test. Three additional specimens were labelled as *100-2CS*, *100-CS* and *100-4CS*, here the *S* indicates a stiffened section (Fig. 1(c)) as will be described. Bolt spacing was kept to 50mm for all specimens. Slenderness ratios of the diaphragm plates can be represented by $\lambda = d/t$, ranged from 24.3 (specimen 100-3C) to 52.8 (specimen 120-2C).

Four control tests of SHS without a diaphragm plate (100-0M, 100-0C, 120-0M and 120-0C) were conducted to identify the contribution of the SHS. Further, in order to investigate the effect of stiffening of the SHS connecting flanges, three additional specimens with stiffened flanges (Fig.1(c)) were fabricated. In these specimens, two pieces of 19.5mm thick mild steel plates were welded to the two connected sides of the SHS.

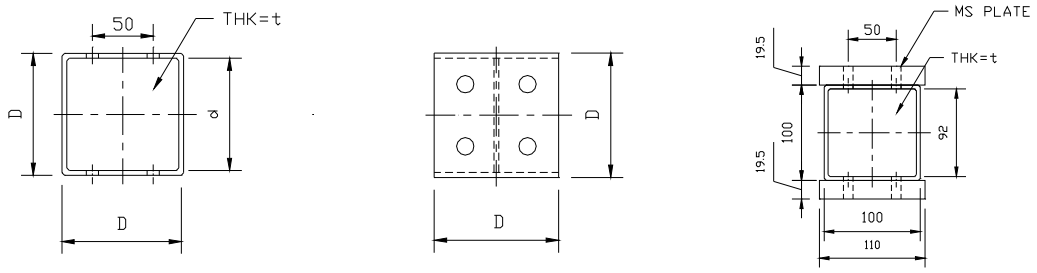

(a) (b) (c)

Figure 1 Yielding Shear Panel Device: (a) Elevation, (b) Top View and (c) Stiffened Specimens

2.4 Test setup and instrumentation

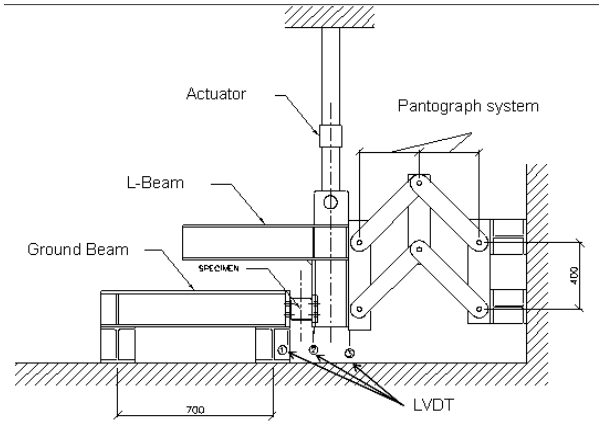

Fig. 2 Test setup

Figure 2 shows a schematic view of the experimental platform used in this study. The test specimens were installed between a ground beam and an L-beam, securely fastened by four M16 bolts (snug tight) on each side. Forced displacement was applied by an MTS 100kN capacity computer-controlled actuator quasi-statically to the specimen via the L-beam. To ensure the verticality of the applied load, a pantograph system was welded to the right hand side of the L-beam. To prevent the L-beam from deflecting out-of-plane, lateral supports (with rollers) were provided (not shown for clarity). However, these supports were later removed as it was noticed that the pantograph system was adequate to prevent the L-girder from deflecting out-of-plane. The complete test setup rested on a reaction frame which was significantly stiffer. The centreline of the actuator implied an eccentricity, e, to the specimen. Prior to testing, a free-run of the setup (i.e. without the specimen installed) was performed, and the result showed that effect of friction and gravity was negligible. The test setup was robust and repeatable, and no visible damage occurred after all tests were carried out.

The loading histories comprised of three ramped cycles at 0.5, 1.0, 3.0, 5.0, 10.0, and 20.0mm amplitudes. Displacements of the specimens were measured independently by a set of LVDT's, marked as 1 through 3 in Figure 2. While LVDT 1 measures the elastic deformation of the support, the difference across LVDT 1 and 2 measured the absolute deformation of the test specimen. With LVDT3 and the distance between LVDT2 and 3 measured, in-plane rotation of the L-beam could be monitored. Material properties of test specimens are listed in Table 1.

Table 1 Material properties for test specimens

Diaphragm Plates	Measured thickness(mm)	Tensile yield strength (N/mm^2)
2mm	1.86	211.3
3mm	2.83	321.3
4mm	3.78	351.2

2.5 Test observations

All monotonic and cyclic tests were completed successfully. The pantograph system effectively maintained the verticality of the force delivery. In-plane rotation of the L-beam were measured (LVDT 2 & 3) and it was found to be negligible. The ground support deflection (LVDT 1) was confirmed to be elastic.

Due to the space limit in this paper only selected cyclic test results are presented. Hystersis curves of cyclic tests are shown in Figure 3. Average shear strain of specimens is defined as $\gamma = \delta / D$, where δ is the difference across LVDT 1 and 2. Specimen 100-2C exhibited reasonably stable hysteresis.

Inelastic shear buckling was noticeable in the last cycle (20mm amplitude) and its effect can be observed from the slightly pinched hysteresis near zero displacement. This correspondes to the buckle forming in the reverse direction. Specimens with thicker diaphragm plates (100-3C and 100-4C) did not show buckling, but demonstrated poor performance as seriously pinched hysteresis loops is recorded (not shown). Significant localised deformation was observed near their connections. It is believed that the local deformations of the SHS have caused the poor performance of these specimens. The 120-2C and 120-3C specimens performed satisfactorily with fairly stable and large force-displacement hysteresis. Both of these specimens have buckled and the effect is visible in their hysteresis loops. Specimen 120-4C demonstrated poor behaviour due to the same reasons discussed above. Specimens with stiffened flanged offered certain improvement when compared to their unstiffened counterpart. The additional mild steel plates have restrained the local deformation of the SHS at their connections.

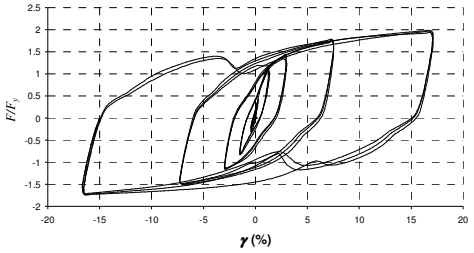

(a) 100-2C

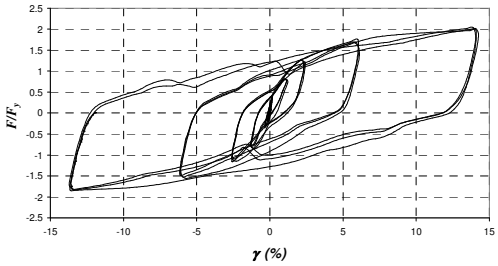

(b) 120-2C

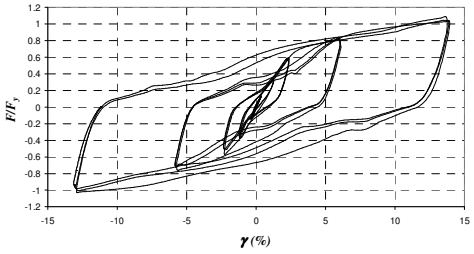

(c) 120-3C

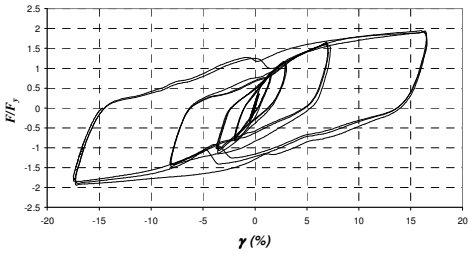

(d) 100-2CS

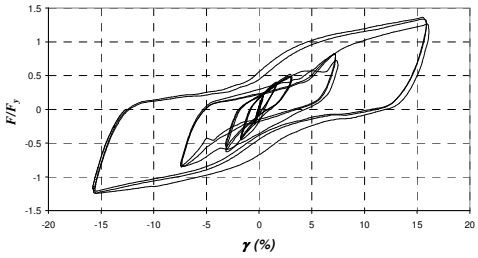

(e) 100-3CS

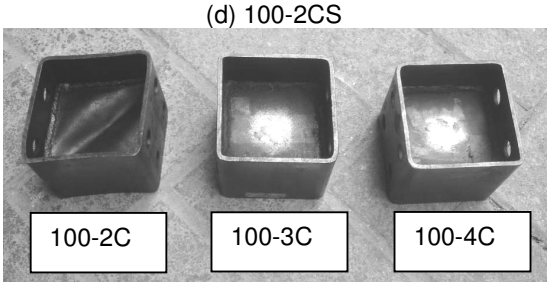

(f) 100mm specimens

Fig. 3 Hysteresis curves and photograph of specimens

3 Energy dissipation, effective stiffness and damping

Cumulative dissipated energy of specimens is shown in Figure 4. The wobbles correspond to the elastic energy release at the unloading path of each cycle. At the end of the test, specimen 100-2C dissipated the largest amount of energy, and at the fastest rate. 120-3C and 120-2C followed closely. 100-2CS dissipated a smaller amount compared to 100-2C, possibly due to the increased eccentricity. To this point, specimen 100-2C offered the best energy dissipative characteristic.

On the other hand, it is generally accepted that energy dissipated in cyclic straining of metals is rate-independent. For practical use it is sometimes more preferable to express the device properties in an equivalent viscous system. This is basically a single degree of freedom oscillator with an equivalent stiffness k_{eff} and damping ratio ζ_{eq}, which are defined as,

$$k_{eff} = \frac{|P_{\max}| - |P_{\min}|}{|\delta_{\max}| - |\delta_{\min}|} \quad \text{and} \quad \zeta_{eq} = \frac{1}{4\pi}\frac{E_D}{E_{S0}} \tag{6) \& (7)}$$

For the equivalent system, ζ_{eq} can be obtained by equating the measured energy dissipated per cycle (E_D) in the experiment to that of a viscously damped oscillator. E_{S0} is the energy stored in an elastic spring with a stiffness k_{eff} and displaced by $\delta_{\max}$. The plots of equivalent damping ratio versus effective stiffness is shown in Figure 5 (for different loading cycles). Each point represents a feasible stiffness and equivalent damping ratio of the device. Effective stiffness decreases as the device undergoes larger displacement. It can be observed that equivalent damping ratios vary approximately inversely with effective stiffness. In general the device can furnish a damping ratio ranges between 10 to 35%.

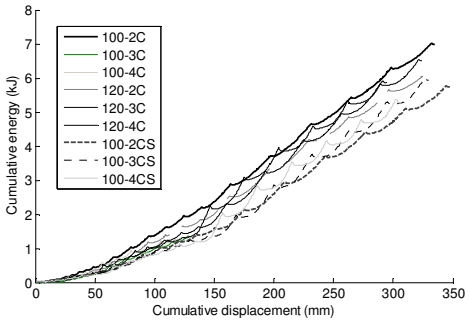

Fig. 4 Cumulative energy dissipation

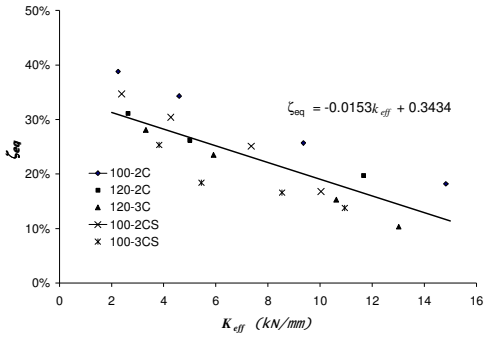

Fig. 5 Equivalent damping ratio and stiffness

4 Numerical example

A continuous Bouc-Wen's model [10] is commonly used by researchers to model the inelastic behavior of passive devices. One single equation governs both elastic and inelastic range of the device under cyclic loading. The restoring force $P(t)$ developed in the device can be expressed by,

$$P(t) = \alpha K_e u(t) + (1-\alpha) K_e u_y z(t) \tag{8}$$

where α is the ratio of post-yield stiffness to the elastic stiffness; K_e is the elastic stiffness of device; $u(t)$ is the displacement; u_y is the yield displacement of device; and $z(t)$ is defined by a first-order nonlinear differential equation which possesses the hysteretic properties,

$$u_y z(t) + \gamma|\dot{u}(t)||z(t)|z(t)|^{n-1} + \beta\dot{u}(t)|z(t)|^n - \dot{u}(t) = 0 \tag{9}$$

γ, β and n are parameters for calibration. Figure 6 shows the Bouc-Wen model as compared to the experimental result of specimen 100-2C.

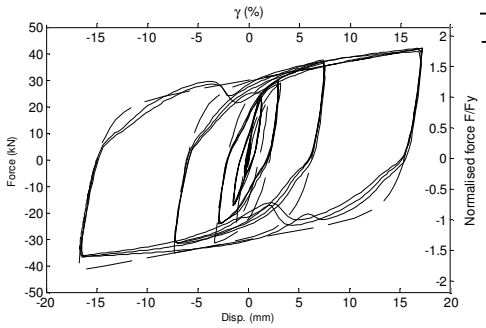

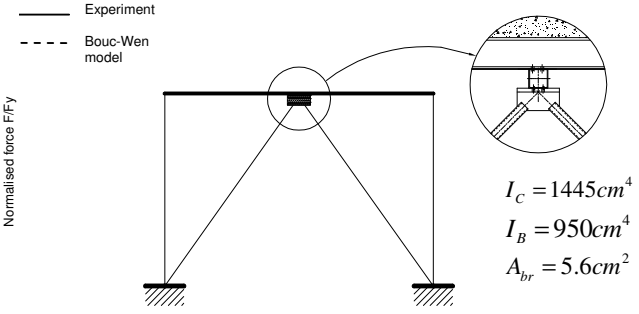

Fig. 6 Bouc-Wen model of 100-2C

Fig. 7 Single story frame retrofitted with YSPD

The model traces the experimental result with reasonable accuracy. To illustrate the benefit of the YSPD, a Bouc-Wen model of the device is now included in the structural model of a single story steel moment frame. Figure 7 shows a single story moment frame retrofitted with a YSPD device fitted on top of a K-brace. It carries a weight of 120kN and its natural frequency is 1.65Hz prior to the addition of the brace and device. The frame is then subjected to the 1940 El Centro North-South ground motion. Figure 8 shows its displacement and velocity responses before and after the retrofit. It is clear that significant reduction in structural response is obtained.

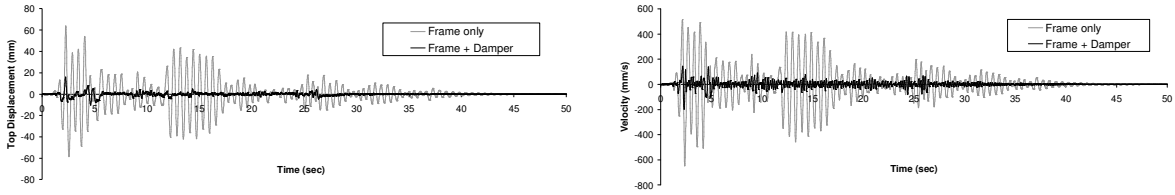

(a) Displacement response (b) Velocity response

Fig. 8 Structural response of single story frame before and after retrofit

5 Conclusions

An experimental study on a new metallic passive energy dissipative device which utilizes plastic shear deformation of steel plate is presented. Major findings are summarized as follows:

1. Devices with large diaphragm plate slenderness exhibited inelastic shear buckling without significant degradation in strength. In particular, the specimen 100-2C with a plate slenderness of 49.5 dissipated the highest amount of energy, and at the highest rate.
2. For devices with thicker plates (smaller slenderness), local deformation of the SHS near its connections were observed, and subsequently offered unsatisfactory energy dissipative capability.
3. A numerical example demonstrated the effectiveness of the proposed device in a damper-brace configuration.

References

[1] Soong TT, Spencer BF Jr, Supplemental energy dissipation: state-of-the-art and state-of-the-practice, Engineering Structures, 24, 243-259, 2002.

[2] Bergman DM and Goel SC, Evaluation of cyclic testing of steel plate devices for added damping and stiffness, Report No. UMCE87-10, The University of Michigan, Ann Arbor, MI, USA, 1987

[3] Tsai K, Chen H, Hong C, and Su Y. Design of steel triangular plate energy absorbers for seimic-resistant construction, Earthquake Spectra, 9(3):505-528, 1993

[4] Chan RWK and Albermani F, Experimental Study of Steel Slit Damper for Passive Energy Dissipation, accepted for publication in Engineering Structures.

[5] Clark PW, Aiken ID, Tajirian F, Kasai K, Ko E and Kimura I, Design procedures for buildings incorporating hysteretic damping devices. In: Proc. Int. Post-SmiRT Conf. Seminar on Seismic Isolation, Passive Energy Dissipation and Active Control of Vibrations of Structures, Cheju, South Korea, 1999

[6] Nakashima M, Strain-hardening behaviour of shear panels made of low-yield steel, I: Test, Journal of Structural Engineering, Vol. 121, No 12, 1742-1749, 1995.

[7] Tanaka K, Torii T, Saski Y, Miyama T, Kawai H, Iwata M et al. Practical application of damage tolerant structures with seismic control panel using low yield point steel to a high-rise steel building. Proceedings, Structural Engineering World Wide, Elsevier, CD-ROM, Paper T190-4, 1998.

[8] Schmidt K, Dorka UE, Taucer F and Magnonette G, Seismic retrofit of a steel frame and an RC frame with HYDE systems, Institute for the Protection and the Security of the Citizen European Laboratory for Structural Assessment, European Commission Joint Research Centre, 2004

[9] Williams MS and Albermani F, Monotonic and cyclic tests on shear diaphragm dissipaters for steel frames, Advanced Steel Construction, 2 (1), pp.1-21, 2006.

[10] Wen YK, Method for random vibration of hysteretic systems, J. Engr. Mech., v.102, pp. 249-263, 1976.